JOURNAL OF PHYSICAL ORGANIC CHEMISTRY, VOL. 10, 647–661 (1997)

SOLVATOCHROMISM OF DYES. PART III.† SOLVATOCHROMISM OF MEROCYANINES IN SOME BINARY MIXTURES OF SOLVENTS. SA–SAB–SB, A NEW MODEL OF SOLVATOCHROMISM

JACEK A. SOROKA* AND KRYSTYNA B. SOROKA

Section of Physical Chemistry, Technical University of Szczecin, PL 71-065 Szczecin, Poland

A quantitative model of solvatochromism in a binary solvent system is presented. Although it is derived for merocyanine and betaine dyes, it explains a majority of known examples of solvatochromism in binary solvents. The model provides an estimation of equilibrium constants between particular types of solvates present therein. UV–VIS absorption spectra of solvated species can be simulated. They perfectly fit the experimental data. The model proposed describes the internal solvent picture from the solute point of view, which differs from other known models and may be useful for studying the structure of liquids. © 1997 John Wiley & Sons, Ltd.

J. Phys. Org. Chem. **10**, 647–661 (1997) No. of Figures: 16 No. of Tables: 6 No. of References: 30

Keywords: merocyanines; solvatochromism; solvent polarity; VBHB model; SA–SAB–SB model; binary solvent mixtures; solvation equilibria; spectra simulation; pyridinium betaines; 7*H*-indolo[1,2-*a*]quinolinium betaines

Received 2 December 1996; revised 7 February 1997; accepted 3 March 1997

INTRODUCTION

Since pyidinium betaine[2] and merocyanine dyes[3,4] show very strong solvatochromism, they have been selected, also in our approach[5–7] to a quantitative interpretation of solvent polarity.[8,9] Recently, we introduced[5,6] a new, consistent and generally valid VBHB model,[1] which provides a qualitative and quantitative treatment of solvatochromism in single solvents. It involves also deep changes induced by a single solvent in the molecular structure of the solute.

In the case of merocyanine dyes, a change of solvent from non-polar to highly polar induces a change in the solute structure which varies from vinylogous amide (V) and its dimers through betaine (B) to hydrogen-bonded betaine (BH). This model is unsuitable for studying solvatochromism in binary solvents. The study of binary solvent mixtures is of great interest, taking into account the possibility of preparing a mixture of a required polarity for real applications. It has generally been accepted that the polarity of a mixture of two similar solvents can be altered smoothly by changes in its composition. The polarity varies linearly with the molar fraction of a given solvent component. However, experiments in which many polarity indicators were used did not show such linearity.[4,10] Many attempts to solve this problem have met with only partial success.

The first, phenomenological well known look at the problem of binary solvent mixtures, presented by Langhals,[11] concerned the analysis of only chosen regions of concentration of solvents and only one dye, i.e. the Dimroth–Reichardt betaine dye. Moreover, the Langhals model introduces an experimental parameter of unclear physical sense.

A further model, based on the proportionality between the Gibbs energy changes connected with the solvatochromic shift and that of the solvent due to the transition from pure solvents to a binary mixture, was proposed by Pytela and Ludwig.[12] In that attempt, the best description of additional Gibbs energy was found when the so-called classical Margules fourth-order equation[13] was used. Another adequate model, supported by physical evidence, was elaborated by Skwierzyński and Connors.[14] This model describes well the interactions between solvents in binary solvent mixtures as intersolvent complex formation. However, the interaction of the solvent with the solute (e.g.

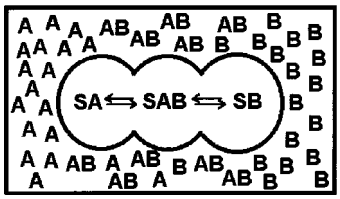

Scheme 1

* *Correspondence to:* J. A. Soroka.

† For Part II, see Ref. 1.

 CCC 0894–3230/97/090647–15 $17.50

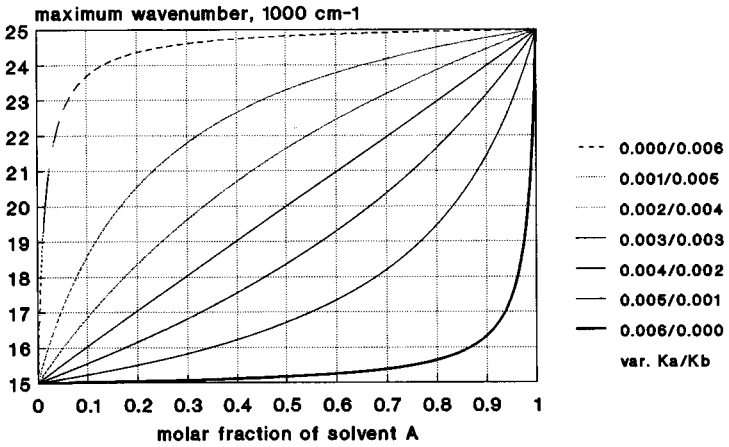

Figure 1. Relationship between the position of the longest wavelength absorption maximum (in 1000 cm^{-1}) and the molar fraction of solvent A, calculated for a molar volume of both solvents of 30 cm^3, ν_{SA}, ν_{SAB} and ν_{SB}=25 000, 20 000 and 15 000 cm^{-1}, respectively, β=0 and variations of K_A and K_B when the sum of both constants remains equal to 0·006. The SA–SB case

solvatochromic indicator) were taken into consideration with less precision (faulty mass balance in the chemical equilibrium equations, inserted into the calculations), and were limited to preferential solvation parameters proposed previously by Dawber *et al*.[15] It is possible to conclude that this model describes the solvatochromism in binary solvent mixtures from the position of the solvents.

The Skwierzyński–Connors model was tested by Rosés and co-workers[16–18] using over 100 binary solvent mixtures, including mixtures showing synergetic properties (mixtures of trialkyl phosphates, dimethyl sulfoxide, acetonitrile and nitromethane with chloroform, alcohols and water). With the last-mentioned mixtures, it was observed that increasing the temperature decreases the intensity of the synergetic effect,[17] indicating the thermal decomposition of the relevant solvent–solvent complexes. In general, the compliance found was high when the two-molecular microspheres were accepted, but the standard deviations (in the original paper[16] expressed in E_T^N units) were sometimes greater than the standard measurements error, even with a medium-class spectrophotometer (20 cm^{-1}; here, after recalculations over 300 cm^{-1}). By means of the application of a five-parameter model [two preferential solvations and three $E_T(30)$ parameters] a good quantitative description of over 70 binary solvent mixtures was possible.[18]

In this paper, we present a description of the solvatochromism in binary solvent systems from the position of the solute, i.e. solvatochromic indicator, using our original model. This model, presented as the third part of our series on solvatochromism theory, was elaborated 10

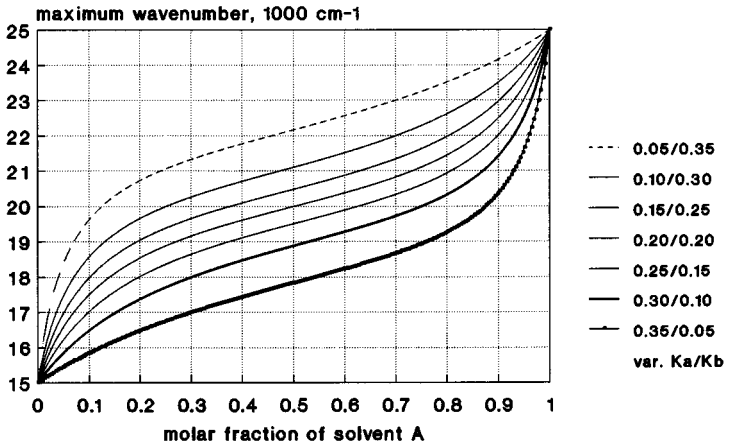

Figure 2. Relationship between the position of the longest wavelength absorption maximum (in 1000 cm^{-1}) and the molar fraction of solvent A, calculated for a molar volume of both solvents of 30 cm^3, ν_{SA}, ν_{SAB} and ν_{SB}=25 000, 20 000 and 15 000 cm^{-1}, respectively, β=0 and variations of K_A and K_B when the sum of both constants remains equal to 0·40. The full SA–SAB–SB case

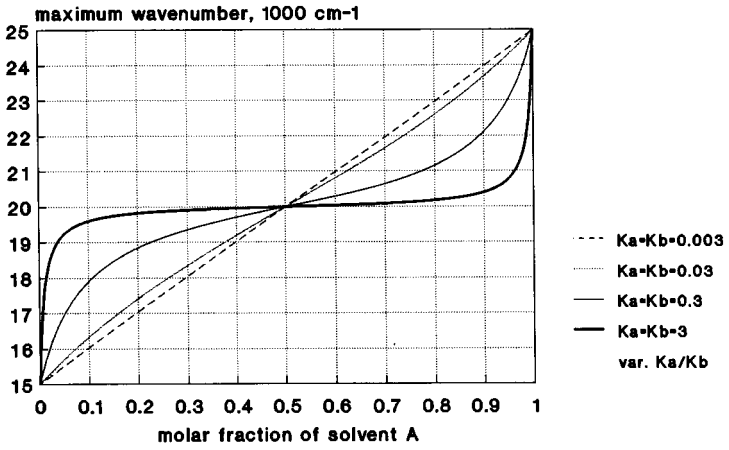

Figure 3. Relationship between the position of the longest wavelength absorption maximum (in 1000 cm^{-1}) and the molar fraction of solvent A, calculated for a molar volume of both solvents of 30 cm^3, ν_{SA}, ν_{SAB} and ν_{SB} = 25 000, 20 000 and 15 000 cm^{-1}, respectively, β = 0, and variations of K_A and K_B constants with $K_A = K_B$

years ago and was successfully applied to explain many experiments results.[6, 19–21] We present here the full version of our model, which is related to a certain extent to the rather simple statistical model of a dipole in an Onsager cavity and is similar to that postulated by Hida *et al*.[22]

DESCRIPTION OF THE MODEL AND ITS VERIFICATION

It is assumed that molecules of two solvents, A and B, do not form stable associates, that molecules of a solute, a dye S, form three three types of solvates, i.e. SA, SAB or SBA, and SB with molecules of both solvents, and that no side-reactions occur.

The following equilibria can be written in such a case:

$$SA + B \underset{k_{-1}}{\overset{k_1}{\rightleftarrows}} SAB \quad (1)$$

$$SB + A \underset{k_{-2}}{\overset{k_2}{\rightleftarrows}} SAB \quad (2)$$

They are additionally illustrated by Scheme 1.

Equilibrium constants are expressed as

$$K_A = \frac{[SAB]}{[SA][B]} \quad (3)$$

$$K_B = \frac{[SAB]}{[SB][A]} \quad (4)$$

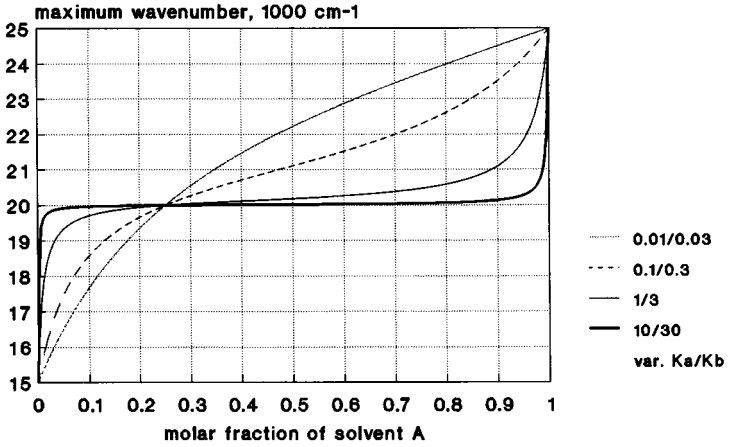

Figure 4. Relationship between the position of the longest wavelength absorption maximum (in 1000 cm^{-1}) and the molar fraction of solvent A, calculated for a molar volume of both solvents of 30 cm^3, ν_{SA}, ν_{SAB} and ν_{SB} = 25 000, 20 000 and 15 000 cm^{-1}, respectively, β = 0, and variations of K_A and K_B when K_B is three times greater than K_A

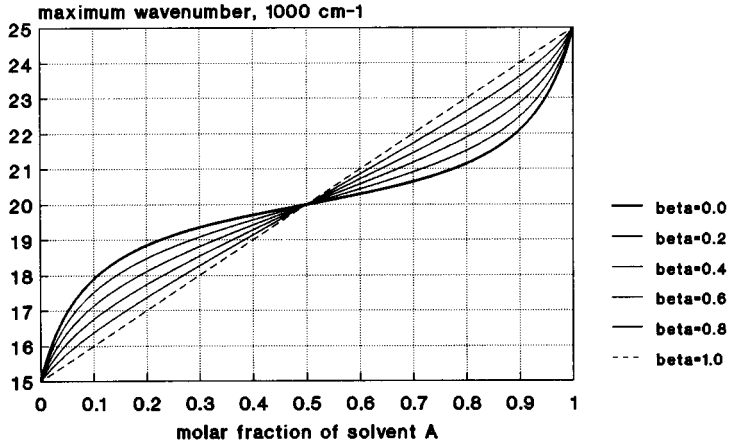

Figure 5. Relationship between the position of the longest wavelength absorption maximum (in 1000 cm^{-1}) and the molar fraction of solvent A, calculated for a molar volume of both solvents of 30 cm^3, ν_{SA}, ν_{SAB} and ν_{SB} = 25 000, 20 000 and 15 000 cm^{-1}, respectively, $K_A = K_B = 0{\cdot}3$ and β varied from 0·0 to 1·0

Under conditions of equilibrium and the absence of side-reactions, the following concentrations can be written:

$$c_S = [SA] + [SAB] + [SB] \quad (5)$$

$$c_A = [SA] + [SAB] + [A] \quad (6)$$

$$c_B = [SB] + [SAB] + [B] \quad (7)$$

Since the concentration of S is negligibly low in comparison with either [A] or [B], equations (6) and (7) can be reduced to

$$c_A = [A] \quad (6a)$$

$$c_B = [B] \quad (7a)$$

The following concentrations of the solvate result from equations (3), (4), (5), (6a) and (7a):

$$[SA] = c_S \cdot \frac{\frac{K_B}{K_A} \cdot \frac{c_A}{c_B}}{\frac{K_B}{K_A} \cdot \frac{c_A}{c_B} + K_B c_A + 1} \quad (8)$$

$$[SAB] = c_s \cdot \frac{K_B c_A}{\frac{K_B}{K_A} \cdot \frac{c_A}{c_B} + K_B c_A + 1} \quad (9)$$

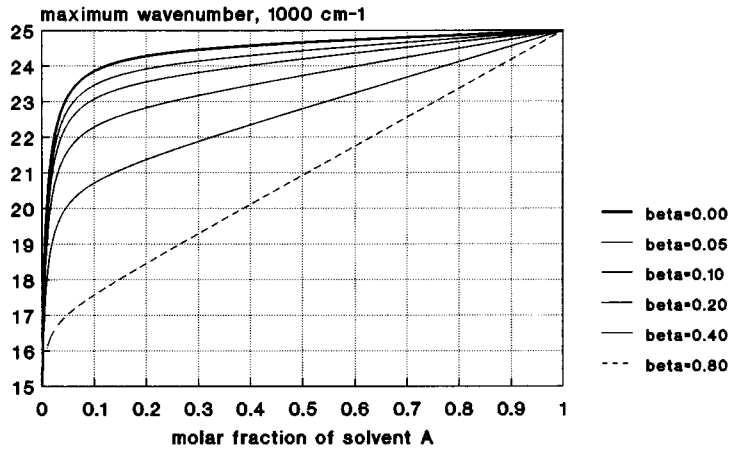

Figure 6. Relationship between the position of the longest wavelength absorption maximum (in 1000 cm^{-1}) and the molar fraction of solvent A, calculated for a molar volume of both solvents of 30 cm^3, ν_{SA}, ν_{SAB} and ν_{SB} = 25 000, 20 000 and 15 000 cm^{-1}, respectively, $K_A = 0{\cdot}003$, $K_B = 0{\cdot}3$ and β varied from 0·0 to 0·80. The SA–SB case

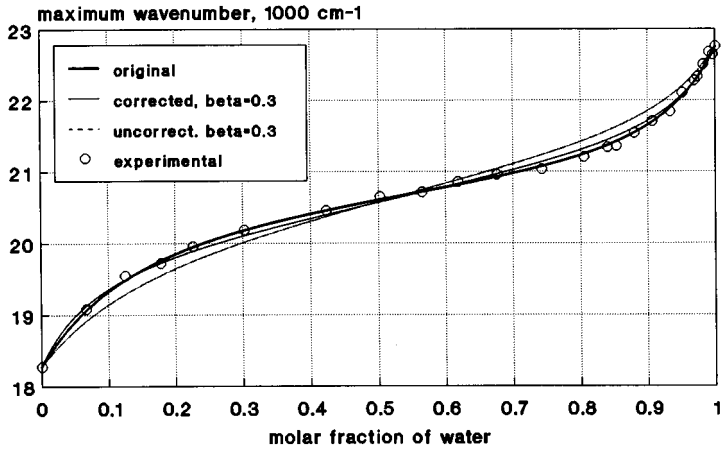

Figure 7. Comparison of experimental data with those calculated for dye **Ij** in acetonitrile–water mixtures at 298·2 K. Particular plots were calculated when original (collected in Table 4, evaluated and applied for $\beta=0$), corrected (evaluated and applied for $\beta=0{\cdot}3$) and uncorrected (evaluated for $\beta=0$ and applied for $\beta=0{\cdot}3$) values of the K_A and K_B parameters were used

$$[\mathrm{SB}] = c_s \cdot \frac{1}{\dfrac{K_B}{K_A} \cdot \dfrac{c_A}{c_B} + K_B c_A + 1} \tag{10}$$

The characteristic transition energies for the particular solvates SA, SAB and SB can be expressed in wavenumbers, $\bar{\nu}_{SA}$, $\bar{\nu}_{SAB}$, and $\bar{\nu}_{SB}$, respectively. The assumption that these transition energies are independent of the polarity of the surrounding medium is not correct. Even if the formation of a solvate compensates for the dipole moment of a solute occurring in the ground state, such compensation fails to occur in the excited state. Hence, the transition energies for particular solvates have to be functions of interactions with the surrounding solvent. As in the first approximate attempt, they are limited solely to the linear term expressed by the equations

$$\bar{\nu}_{SA} = \bar{\nu}^0_{SA} + \beta(1-x)(\bar{\nu}^0_{SB} - \bar{\nu}^0_{SA}) \tag{11}$$

$$\bar{\nu}_{SAB} = \bar{\nu}^0_{SAB} + \beta[\bar{\nu}^0_{SB}(1-x) + x\bar{\nu}^0_{SA} - \bar{\nu}^0_{SAB}] \tag{12}$$

$$\bar{\nu}_{SB} = \bar{\nu}^0_{SB} + \beta x(\bar{\nu}^0_{SA} - \bar{\nu}^0_{SB}) \tag{13}$$

where x is the molar fraction in the mixture with solvent B and all $\bar{\nu}^0_{SA}$, $\bar{\nu}^0_{SAB}$ and $\bar{\nu}^0_{SB}$ are wavenumbers of absorption maxima independent of the environment and β is a parameter without dimension, characterizing the polarities of all solvates. In the first approximation, accepted in this paper, β is common for all of the solvates SA, SAB and

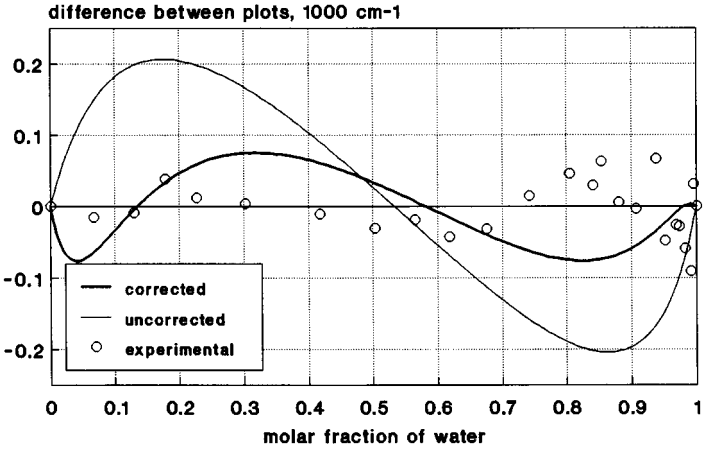

Figure 8. Differences between experimental and calculated data for dye **Ij** in acetonitrile–water mixtures at 298·2 K. Particular plots concerned situations when original (collected in Table 4, evaluated and applied for $\beta=0$), corrected (evaluated and applied for $\beta=0{\cdot}3$) and uncorrected (evaluated for $\beta=0$ and applied for $\beta=0{\cdot}3$) values of the K_A and K_B parameters were used

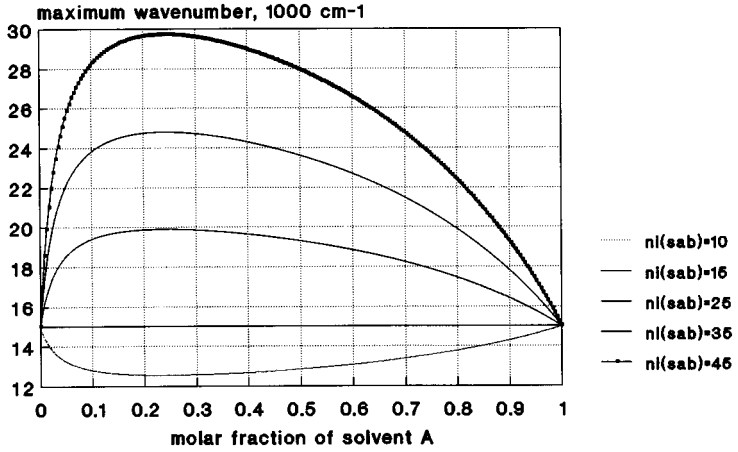

Figure 9. Relationship between the position of the longest wavelength absorption maximum (in 1000 cm^{-1}) and molar the fraction of solvent A, calculated for a molar volume of both solvents of 30 cm^3, ν_{SA} and ν_{SB} = 15 000 cm^{-1}, K_A = 0·05, K_B = 0·5, β = 0 and ν_{SAB} varied. The situation of the so-called synergetic effect, when the energy of transition of the mixed solvate exceeds that of the simple solvates

SB.

Because all $\bar{\nu}_{SA,\,SAB,\,SB}$ values depend on the environment, the $\bar{\nu}^0_{SA,\,SAB,\,SB}$ values should be understood as the magnitudes expected in binary mixtures with A:B ratios of 1:0, 1:1 and 0:1, respectively.

The affinity of these transition energies to the environmental effects is characterized by the β parameter. Thus, if β=0, which is understood as the lack of interactions in the ground state, the $\bar{\nu}$ magnitudes in equations (11)–(13) are equal to the $\bar{\nu}_0$ magnitudes.

The value β=1 means that a solvate interacts equally strongly with a medium as does a solute. In this circumstance, two extreme cases can be distinguished, for x=0 and x=1. Thus, for β=1 and x=0,

$$\bar{\nu}_{SA} = \bar{\nu}_{SAB} = \bar{\nu}_{SB} = \bar{\nu}^0_{SB} \tag{14a}$$

and for β=1 and x=1,

$$\bar{\nu}_{SA} = \bar{\nu}_{SAB} = \bar{\nu}_{SB} = \bar{\nu}^0_{SA} \tag{14b}$$

In real situations, β is bottom and upper limited, i.e. $0<\beta<1$, and when β=1 the $\bar{\nu}$–x relation is reduced to a straight line varying from $\bar{\nu}^0_{SB}$ to $\bar{\nu}^0_{SA}$.

The location of the maximum absorption band, composed of three ones, may be calculated according to the method described previously.[5,7] This method concerned the case of closely positioned overlapping absorption bands, which can

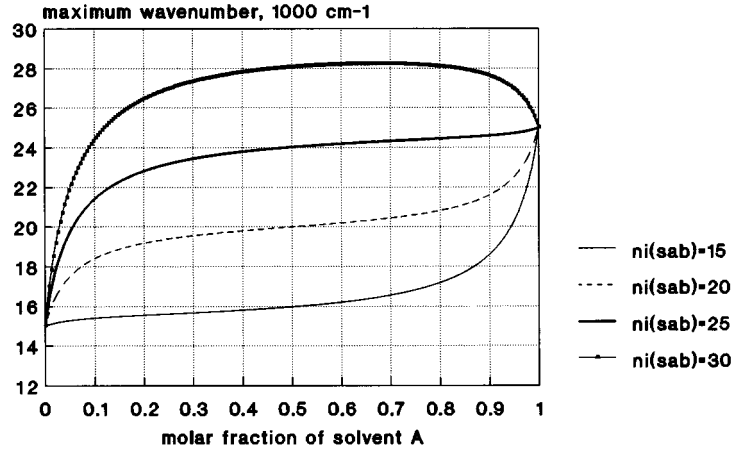

Figure 10. Relationship between the position of the longest wavelength absorption maximum (in 1000 cm^{-1}) and the molar fraction of solvent A, calculated for a molar volume of both solvents of 30 cm^3, ν_{SA} and ν_{SB} = 25 000 and 15 000 cm^{-1}, respectively, equilibrium constants $K_A = K_B$ = 0·5, β = 0 and ν_{SAB} varied. The situation of the so-called synergetic effect, when the energy of transition of the mixed solvate exceeds that of the simple solvates

be satisfactorily approximated to a Gaussian curve. The shape of the envelope composed of three Gaussian functions is expressed by

$$W=\sum_{i=1}^{3}[A_i]\varepsilon_i \exp\left[-\frac{(\bar{\nu}-\bar{\nu}_i)^2}{2\sigma_i^2}\right] \tag{15}$$

where ε_i and σ_i denote the molar extinction coefficient and the half-width of the absorption band, respectively. The maximum of this envelope becomes available under the condition

$$\frac{\partial W}{\partial \bar{\nu}}=0 \tag{16}$$

It gives a non-explicit form of the solution:

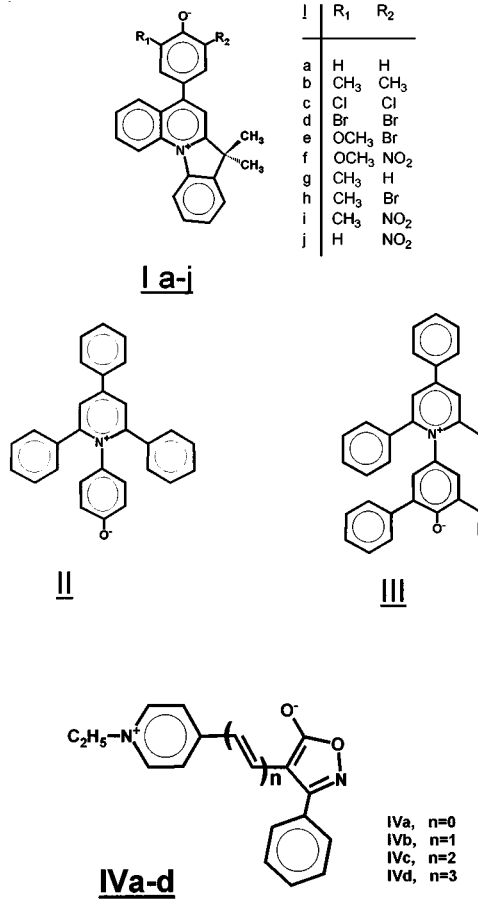

I	R_1	R_2
a	H	H
b	CH_3	CH_3
c	Cl	Cl
d	Br	Br
e	OCH_3	Br
f	OCH_3	NO_2
g	CH_3	H
h	CH_3	Br
i	CH_3	NO_2
j	H	NO_2

Scheme 2

$$\sum_{i=1}^{3}\frac{\varepsilon_i}{\sigma_i^2}[A_i](\bar{\nu}-\bar{\nu}_i)\exp\left[-\frac{(\bar{\nu}-\bar{\nu}_i)^2}{2\sigma_i^2}\right]=0 \tag{17}$$

If the bands which constitute the envelope are either sufficiently broad (large value of σ) or they overlap, the following condition is fulfilled:

$$\left|\frac{\bar{\nu}-\bar{\nu}_i}{\sigma_i}\right| \ll 1 \tag{18}$$

and hence

$$\frac{(\bar{\nu}-\bar{\nu}_i)^2}{2\sigma_i^2}\approx 0 \tag{19}$$

In such a case, equation (17) takes the simpler form

$$\sum_{i=1}^{3}\frac{\varepsilon_i}{\sigma_i^2}[A_i](\bar{\nu}-\bar{\nu}_i)=0 \tag{20}$$

and the position of the maximum is given by

$$\bar{\nu}=\frac{\sum_{i=1}^{3}\frac{\varepsilon_i}{\sigma_i^2}[A_i]\bar{\nu}_i}{\sum_{i=1}^{3}\frac{\varepsilon_i}{\sigma_i^2}[A_i]} \tag{21}$$

In our case, the following equation is derived:

$$\bar{\nu}=\frac{\frac{\varepsilon_{SA}}{\sigma_{SA}^2}[SA]\bar{\nu}_{SA}+\frac{\varepsilon_{SAB}}{\sigma_{SAB}^2}[SAB]\bar{\nu}_{SAB}+\frac{\varepsilon_{SB}}{\sigma_{SB}^2}[SB]\bar{\nu}_{SB}}{\frac{\varepsilon_{SA}}{\sigma_{SA}^2}[SA]+\frac{\varepsilon_{SAB}}{\sigma_{SAB}^2}[SAB]+\frac{\varepsilon_{SB}}{\sigma_{SB}^2}[SB]} \tag{22}$$

If the volume contraction of mixing of two solvents is neglected, the relationship between the molar fraction of the solvent A and its molarity is given by the following equations:

$$c_A=\frac{x}{x\cdot\frac{M_A}{\rho_A}+(1-x)\frac{M_B}{\rho_B}} \tag{23}$$

$$c_B=\frac{1-x}{x\cdot\frac{M_A}{\rho_A}+(1-x)\frac{M_B}{\rho_B}} \tag{24}$$

where M_A and M_B are the molecular weights of solvents A and B, respectively, and ρ_A and ρ_B are their densities. Equations (8)–(24) represent the complete mathematical model of solvatochromism in binary solvent systems.

PROPERTIES OF THE MODEL DISCUSSED

In the case when both equilibrium constants, K_a and K_b, have small values, the model describes simple exchange. This situation is presented in Figure 1, in which theoretical curves are connected with variable K_A and K_B values when the sum of K_A and K_B remains constant (0·006 here).

A similar situation, but calculated for higher values of the equilibrium constants (here the sum of both constants is equal to 0·40) is presented in Figure 2. In this case, the presence of a SAB solvate is readily visible.

The role of the K_A and K_B values in the case when they are equal and not equal is presented in Figures 3 and 4, respectively.

Consecutive pictures show the influence of the β parameter. In Figures 5 and 6 the particular equilibrium constants are equal and not equal, respectively. The effect of the β parameter in the case of dye **Ij** in acetonitrile–water solvent system at 298·2 K is presented in Figures 7 and 8. Both pictures show the situation when proper (both evaluated and applied for $\beta=0$ and $\beta=0{\cdot}3$, respectively) and improper (evaluated for $\beta=0$ but applied for $\beta=0{\cdot}3$) values of K_A and K_B were used. The differences between the relevant plots and experimental data are presented in Figure 8.

Figures 9 and 10 show the so-called synergetic effect. Calculations were performed for equal (Figure 9) and unequal (Figure 10) locations of the absorption maxima of SA and SB solvates. In Figure 9, the effect of negative and positive synergism is visible, but in Figure 10 only positive synergism.

VERIFICATION OF THE MODEL

Using a set of solvatochromic dyes, this model was verified in two independent ways.

In the first method, the K_A and K_B constants and $\bar{\nu}_{SAB}$, values experimentally determined for merocyanine dyes **Ia**–**j** and betaine **II** (see Scheme 2) in two binary solvent systems (pyridine monohydrate–water and acetonitrile–water), were applied. The experimental data from UV–VIS spectral measurements are given in Tables 1–3. They fit this model perfectly, even under the assumptions that $\beta=0$ and

$$\frac{\varepsilon_{SA}}{\sigma^2_{SA}}=\frac{\varepsilon_{SAB}}{\sigma^2_{SAB}}=\frac{\varepsilon_{SB}}{\sigma^2_{SB}} \tag{25}$$

The characteristics of this adjustment and the parameters of the relationships found are given in Table 4 and Figure 11.

The experimental data for compound **III** and compounds **IVa**–**d** (Scheme 3) are taken from other sources.[4, 10] They represent classical examples of solvatochromism. The

Table 1. Position[a] of the $S_1 \leftarrow S_0$ bands of dyes **Ia**–**j** in pyridine monohydrate–water solutions at 25±0·1 °C

	Dyes									
x_{H_2O}[b]	**Ia**	**Ib**	**Ic**	**Id**	**Ie**	**If**	**Ig**	**Ih**	**Ii**	**Ij**
0·000	17·60	16·66	17·75	17·77	16·60	17·99	17·13	17·08	18·20	19·08
0·058	17·75	16·70	17·86	17·76	16·64	18·10	17·17	17·12	18·28	19·04
0·148	17·93	16·76	18·03	17·99	16·80	18·16	17·30	17·28	18·44	19·38
0·222	18·08	16·84	18·08	18·00	16·88	18·20	17·42	17·34	18·52	19·46
0·284	18·21	16·90	18·28	18·23	17·00	18·22	17·50	17·48	18·67	19·50
0·338	18·30	16·96	18·37	18·30	17·08	18·28	17·58	17·54	18·74	19·64
0·428	18·52	17·12	18·62	18·43	17·22	18·36	17·79	17·72	18·99	19·82
0·524	18·70	17·24	18·78	18·67	17·40	18·66	18·11	17·92	19·16	20·02
0·636	18·91	17·42	18·92	18·83	17·57	18·82	18·14	18·10	19·35	20·16
0·726	19·13	17·56	19·26	19·04	17·78	19·00	18·32	18·28	19·50	20·34
0·780	19·24	17·64	19·34	19·14	17·92	19·12	18·44	18·38	19·67	20·48
0·800	19·30	17·74	19·44	19·16	17·96	19·18	18·52	18·44	19·72	20·52
0·836	19·40	17·89	19·50	19·34	18·06	19·30	18·59	18·54	19·83	20·74
0·874	19·56	17·94	19·64	19·52	18·18	19·38	18·71	18·68	19·97	20·84
0·914	19·72	18·14	19·84	19·65	18·40	19·60	18·92	18·96	20·17	20·97
0·936	19·90	18·24	20·01	19·85	18·54	19·74	19·11	19·08	20·28	21·10
0·956	20·10	18·50	20·25	20·07	18·78	19·92	19·22	19·30	20·55	21·26
0·968	20·30	18·70	20·41	20·32	18·94	20·08	19·29	19·42	20·70	21·38
0·978	20·54	18·96	20·66	20·46	19·18	20·30	19·68	19·72	20·88	21·49
0·990	20·80	19·24	20·97	20·73	19·54	20·72	19·99	20·06	21·22	21·78
0·996	21·06	19·48	21·24	21·04	19·80	21·44	20·23	20·32	21·49	22·20
0·998	21·12	19·62	21·29	21·13	19·90	21·66	20·34	20·42	21·58	22·46
1·000	21·26	19·70	21·42	21·24	20·00	22·26	20·50	20·56	21·75	22·72

[a] As $\bar{\nu}_{max}$, 1000 cm^{-1}.
[b] Molar fraction of water.

interpretation of the relevant data gave the results presented in Table 5.

Figure 11 illustrates, among other things, the application of our model to the data found by Dimroth and Reichardt[10] for betaine **III** in the pyridine–water system at 298·2 K. Also presented is the application of our model when a stable hydrate of pyridine was not taken into account [Figure 11(c)]. In some ranges of the molar fraction of water therein, the deviations of the experimental points from the curve predicted by the model are systematic. Between 0 and 0·3 and between 0·75 and 0·95 mol mol^{-1} the deviations are positive, and in the range from 0·35 to 0·65 mol mol^{-1} they are negative. The existence of pyridine monohydrate as a stable complex implies two binary subsystems: pyridine–pyridine monohydrate and pyridine monohydrate–water. Such an assumption is useful [cf. Figure 11(d)]. The systematic deviations vanish, apart from some stochastic deviations with an amplitude not higher than the experimental error. At this point it seems important to emphasize that systematic deviations of the experimental data from those predicted by our model indicate the existence of relatively stable intersolvent complexes which should not be neglected.

The second method of verification of the model presented is based on the set of results $\{\bar{\nu}, \varepsilon, x_i\}$ for a chosen merocyanine dye (here **Ie**). These data are involved in a simulation of the UV–VIS spectra at 298·2 K for $0{\cdot}4 \leq x \leq 1$ molar fractions of water in pyridine monohydrate. Based on the calculated values of all $\bar{\nu}_{SAB}$, K_A and K_B, the spectra were simulated and then compared with the experimental spectra. The simulated and experimental spectra are very similar, as shown in Figure 12

Figure 13 shows the simulated UV–VIS absorption band of dye **Ie** in solution for $x = 0{\cdot}8$ molar fraction of water with visualization of the constituent bands corresponding to solvates SA, SAB and SB.

Figure 14 presents the positions and relative intensities of the constituent bands corresponding to SA, SAB and SB solvates at various molar fractions of water for the cases shown in Figure 12.

Table 2. Positions[a] of the $S_1 \leftarrow S_0$ bands for dye **Ij** in acetonitrile–water solutions at different temperatures

	T (K)					
x_{H_2O}	288·2	298·2	308·2	318·2	328·2	338·2
0·000	18·18	18·27	18·18	18·23	18·21	18·16
0·068	19·14	19·08	18·97	18·92	18·84	18·78
0·127	19·52	19·52	19·34	19·28	19·15	19·10
0·179	19·78	19·72	19·64	19·54	19·43	19·36
0·225	19·97	19·94	19·80	19·72	19·60	19·54
0·303	20·22	20·18	20·04	19·97	19·92	19·82
0·421	20·44	20·46	20·36	20·26	20·22	20·15
0·504	20·60	20·64	20·50	20·45	20·40	20·36
0·566	20·72	20·74	20·66	20·58	20·54	20·50
0·617	20·80	20·86	20·74	20·64	20·62	20·54
0·675	20·90	20·96	20·80	20·76	20·72	20·64
0·744	20·99	21·06	20·94	20·90	20·85	20·75
0·803	21·16	21·20	21·10	21·06	20·98	20·92
0·839	21·32	21·34	21·24	21·20	21·12	21·02
0·853	21·36	21·36	21·28	21·28	21·18	21·16
0·879	21·55	21·54	21·44	21·38	21·30	21·30
0·906	21·72	21·70	21·62	21·52	21·45	21·40
0·936	21·94	21·86	21·82	21·78	21·66	21·60
0·951	22·10	22·10	21·94	21·88	21·79	21·72
0·967	22·27	22·28	22·12	22·06	21·93	21·88
0·975	22·36	22·34	22·21	22·14	22·01	21·92
0·983	22·46	22·50	22·31	22·21	22·07	22·03
0·991	22·58	22·68	22·38	22·28	22·22	22·14
0·997	22·64	22·64	22·46	22·36	22·30	22·16
0·998	22·65	22·64	22·50	22·47	22·31	22·24
1·000	22·73	22·76	22·54	22·46	22·36	22·26

[a] As $\bar{\nu}_{max}$, 1000 cm^{-1}.

Table 3. Positions[a] of the $S_1 \leftarrow S_0$ bands for dye **II** in pyridine monohydrate–water solutions at different temperatures

	T (K)					
x_{H_2O}	298·2	303·2	308·2	318·2	328·2	338·2
0·000	20·60	20·58	20·34	20·60	20·52	20·89
0·058	20·66	20·76	20·62	20·70	20·65	20·96
0·222	21·26	21·13	21·08	21·05	20·92	21·14
0·338	21·44	21·36	21·28	21·28	21·02	21·29
0·428	21·60	21·60	21·50	21·38	21·30	21·41
0·524	21·74	21·74	21·71	21·58	21·44	21·54
0·636	21·89	21·92	21·87	21·84	21·71	21·68
0·726	22·10	22·12	22·02	21·98	21·88	21·88
0·780	22·24	22·25	22·18	22·08	21·96	22·06
0·800	22·25	22·30	22·22	22·12	22·12	22·14
0·836	22·28	22·38	22·34	22·24	22·12	22·18
0·874	22·42	22·51	22·47	22·36	22·24	22·22
0·914	22·58	22·66	22·61	22·57	22·46	22·44
0·936	22·76	22·89	22·80	22·68	22·66	22·64
0·956	23·00	23·04	23·00	22·96	22·86	22·78
0·968	23·20	23·31	23·18	23·16	23·08	22·92
0·978	23·34	23·39	23·34	23·30	23·24	23·16
0·990	23·58	23·54	23·54	23·60	23·40	23·34
0·996	23·74	23·69	23·70	23·76	23·60	23·50
0·998	23·70	23·78	23·78	23·80	23·64	23·52
1·000	23·80	23·82	23·83	23·88	23·72	23·62

[a] As $\bar{\nu}_{max}$, 1000 cm^{-1}.

DISCUSSION

The results presented allow us to assume that the model under discussion is accurate. The experimental UV–VIS spectra were better simulated (e.g. for dye **Ie**) when the parameter $\beta = 0{\cdot}30$ was accepted. This indicates that the formation of a solvate in the first coordination zone of solvation, connected with one or two molecules of solvent, reduces the interaction with the medium by about 70%.

It seems that pairing of electrons differing in spin in the ground states of chemical compounds, pairing electrons in the form of so-called Cooper's pairs which play a very

important role in classical superconducting materials, pairing humans leading to the creation of families, the discussed pairing of the solute with one molecule of solvent, and many other examples of pairing are one of the important general rules of nature.

The values of the equilibrium constants found approximate to the typical constants characterizing solvent–solvent interactions estimated by the Benesi–Hildebrandt method.[21] The values of entropy and enthalpy change under equilibrium conditions have been found from the $\log K - 1/T$ correlation assuming an interpretation in agreement with the Arrhenius equation. The results obtained are presented in Table 6.

The values of the constants K_A for both the acetonitrile–water and pyridine monohydrate–water systems hardly depend on temperature, which leads to low values of the correlation coefficients. This means, in the framework of the model discussed, that the degree of coordination and energies of solvates SA and SAB are similar. This proves that in both solvates the predominant element is solvent A (in these cases water), which agrees with the observations of many other workers. According to the proposed model, the constants K_A characterize the coordination process of a solvent molecule by an existing dye hydrate. The same conclusions were first drawn by Hida *et al.*[22] during investigations of the solvatochromism of nitroaniline and merocyanine dye derivatives of benzo[*a*]quinolizine. The influence of acetonitrile on the energy of the dye hydrate is insignificant. The situation is different in the case of pyridine monohydrate. One can assume that pyridine monohydrate can be additionally attracted to a dye molecule by ring π electrons whereas acetonitrile does not have this possibility. The effect of temperature on K_B characterizes the process of water molecule addition to the present dye solvate. The entropy changes in this case are insignificant, which means that the structures of both solvates are similar. The significant change in enthalpy proves the strong effect of water on the solvate energy. The substituent effect of the dyes **Ia**–**j** on the estimated K_A and K_B constants in the pyridine monohydrate–water system was attempted using Charton's LDS equation:[24]

$$\log K = L\sum\sigma_I + D\sum\sigma_R^0 + S\sum\nu + H \qquad (26)$$

where *L*, *D* and *S* denote localized charge effect (inductive), donating effect (resonance) and steric interaction, respectively. The correlations obtained were very poor. A better correlation involved the K_A constant set and led to the equation

Table 4. Parameters, estimated according to the SA–SAB–SB model ($\beta = 0$), and their statistical characteristics

Solvent system	Dye	Temperature (K)	Longest wavelength absorptions (1000 cm^{-1}) $\bar{\nu}_{SA}$	$\bar{\nu}_{SAB}$	$\bar{\nu}_{SB}$	K_A (l mol^{-1})	K_B (l mol^{-1})	n	s (1000 cm^{-1})	R[a]
Pyridine monohydrate–water[b]	**Ia**	298·2	21·26±0·10	19·18±0·13	17·60±0·05	0·350±0·059	0·086±0·035	23	0·021	0·9$_4$9
	Ib	298·2	19·70±0·10	17·32±0·17	16·66±0·05	0·301±0·057	0·057±0·017	23	0·035	0·9$_3$8
	Ic	298·2	21·42±0·10	19·50±0·20	17·75±0·05	0·359±0·056	0·066±0·016	23	0·039	0·9$_4$8
	1d	298·2	21·24±0·10	19·32±0·42	17·77±0·05	0·333±0·068	0·054±0·011	23	0·047	0·9$_7$7
	Ie	298·2	20·00±0·10	17·99±0·17	16·60±0·05	0·361±0·044	0·057±0·011	23	0·020	0·9$_4$9
	If	298·2	22·26±0·10	20·78±0·43	17·99±0·05	1·345±1·61	0·0253±0·0039	23	0·046	0·9$_7$7
	Ig	298·2	20·50±0·10	18·00±0·45	17·13±0·05	0·342±0·13	0·099±0·080	23	0·081	0·9$_4$4
	Ih	298·2	20·56±0·10	18·08±0·37	17·08±0·05	0·316±0·076	0·072±0·026	23	0·040	0·9$_3$9
	Ii	298·2	21·75±0·10	20·17±0·16	18·20±0·05	0·498±0·057	0·056±0·011	23	0·031	0·9$_6$9
	Ij	298·2	22·72±0·10	21·63±0·41	19·08±0·05	1·295±1·39	0·0488±0·0083	23	0·056	0·9$_4$6
Acetonitrile–water[c]	**Ij**	288·2	22·73±0·10	19·64±0·26	18·18±0·05	0·0994±0·040	0·280±1·05	26	0·033	0·9$_6$9
	Ij	298·2	22·76±0·10	20·12±0·40	18·27±0·15	0·125±0·090	0·226±1·03	26	0·044	0·9$_4$8
	Ij	308·2	22·54±0·10	19·82±0·17	18·18±0·05	0·0989±0·020	0·203±0·26	26	0·030	0·9$_7$9
	Ij	318·2	22·46±0·10	19·78±0·33	18·23±0·05	0·0943±0·050	0·172±0·52	26	0·027	0·9$_7$9
	Ij	328·2	22·36±0·10	20·26±0·13	18·21±0·05	0·122±0·020	0·147±0·095	26	0·027	0·9$_7$9
	Ij	338·2	22·26±0·10	20·01±0·26	18·16±0·05	0·103±0·040	0·142±0·23	26	0·038	0·9$_4$8
Pyridine monohydrate–water[d]	**Il**	298·2	23·80±0·10	21·26±0·43	20·60±0·05	0·187±0·066	0·151±0·30	21	0·055	0·9$_4$7
	Il	303·2	23·82±0·10	21·36±0·26	20·58±0·05	0·165±0·029	0·110±0·084	21	0·038	0·9$_6$9
	Il	308·2	23·83±0·10	21·47±0·12	20·43±0·05	0·203±0·020	0·127±0·053	21	0·024	0·9$_7$9
	Il	318·2	23·88±0·10	21·48±0·18	20·60±0·05	0·223±0·025	0·0949±0·035	21	0·032	0·9$_7$9
	Il	328·2	23·72±0·10	21·58±0·31	20·52±0·05	0·200±0·031	0·0671±0·025	21	0·048	0·9$_4$8
	Il	338·2	23·62±0·10	21·95±0·29	20·89±0·05	0·228±0·059	0·0473±0·024	21	0·040	0·9$_5$9

[a] Shortened form of curvilinear correlation coefficient, e.g. $0{\cdot}9_48 = 0{\cdot}99998$.
[b] The molar fraction of water (X_{H_2O}) varied from 0 to 1 in 23 consecutive runs.
[c] The molar fraction of water varied from 0 to 1 in 26 consecutive runs.
[d] The molar fraction of water varied from 0 to 1 in 21 consecutive runs.

$$\log K_A = (0{\cdot}49 \pm 0{\cdot}13)\sum\sigma_I + (0{\cdot}35 + 0{\cdot}06)\sum\sigma_R^0 - (0{\cdot}22 \pm 0{\cdot}08)\sum\nu - 0{\cdot}30 \pm 0{\cdot}06 \qquad (27)$$

$$R = 0{\cdot}7611; \qquad n = 10; \qquad 1/\alpha = 36$$

The most significant parameters in this equation were connected with inductive and resonance effects. The correlation of $\log K_B$ with the substituent constants was worse ($R = 0{\cdot}6908$, $n = 10$, $1/\alpha = 16$). On this basis, one can put forward the hypothesis that the geometry of the solvate is to some extent defined. According to this hypothesis, pyridine monohydrate coordinates with the phenol ring modified by substituents. The verification of this hypothesis, however, could only be possible when the determination of the equilibrium constants is more precise and also when some simplifications to the proposed model can be removed. Moreover, the real values of the β parameter should be taken.

The model presented is (to our knowledge) the first successful attempt at a $\bar{\nu} - x$ relationship reconstruction over the full range of concentrations, because it was formulated in its general form several years ago.[6, 19–21] This model, although oversimplified, enables many observations of such experimental results which up to now have not been taken into consideration. It is worth emphasizing that the determined polarities of mixed solvents are useless. As revealed by our experimental data, these polarities, expressed in E_T or other units, are mostly a function of the solvatochromic dye used together with the solvent system studied and not solely of the solvent system. Similar conclusions can be drawn from the papers of Marcus and Migron[25, 26] concerning a variety of solvatochromic indica-

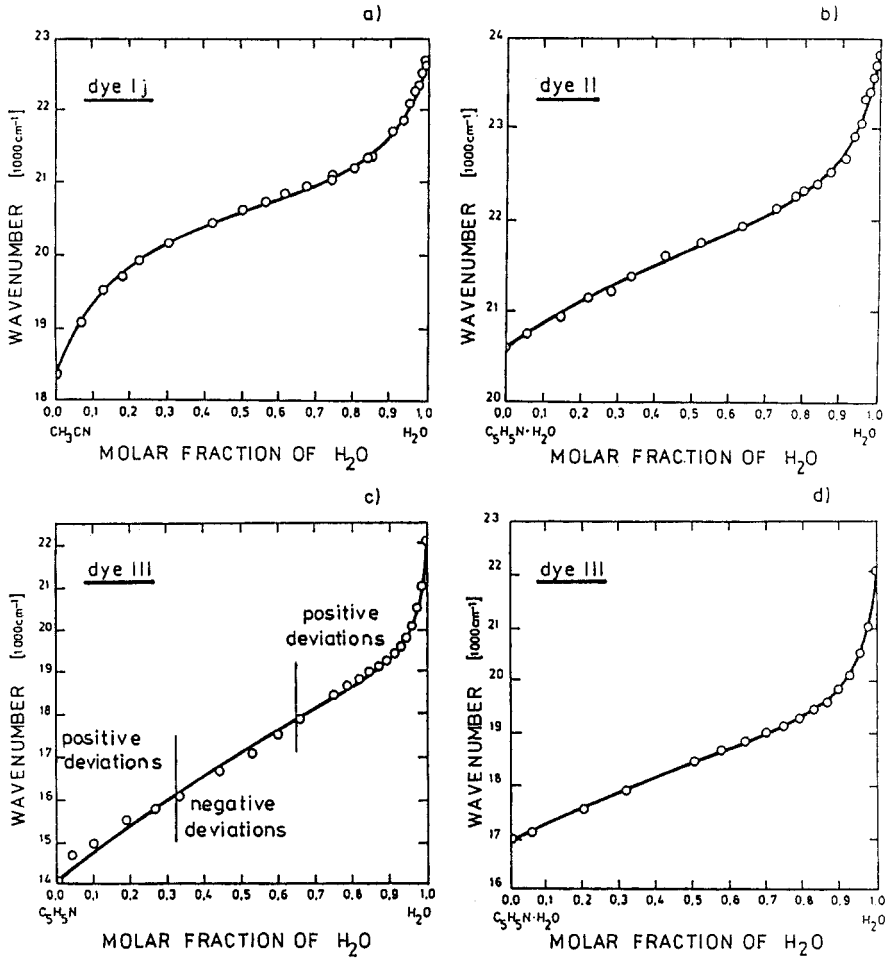

Figure 11. Relationship between the position of the longest wavelength absorption maximum (in 1000 cm^{-1}) and the molar fraction of water, temperature 298·2 K, for (a) merocyanine dye **Ij** in the acetonitrile–water system, (b) betaine dye **II** in the pyridine monohydrate–water subsystem. (c) betaine dye **III** in the pyridine–water system and (d) betaine dye **III** in the pyridine monohydrate–water subsystem

Table 5. Parameters estimated according to the SA–SAB–SB model (β=0), based on $S_1 \leftarrow S_0$ transition wavenumbers at 298 K[a]

Solvent system	Dye	$\bar{\nu}_{SA}$ (1000 cm^{-1})	$\bar{\nu}_{SAB}$ (1000 cm^{-1})	$\bar{\nu}_{SB}$ (1000 cm^{-1})	K_A (l mol^{-1})	K_B (l mol^{-1})	n[b]	S (1000 cm^{-1})	R[c]	Ref.
Pyridine monohydrate–water	**III**	22·08	18·86	16·95	0·3005	0·0929	17	0·037	0·990	8
Piperidine–water	**III**	22·08	17·32	12·42	0·3242	0·1207	21	0·140	0·998	8
2,6-Lutidine monohydrate–water	**III**	22·08	17·97	16·37	0·8671	0·2159	18	0·042	0·998	8
α-Picoline monohydrate–water	**III**	22·08	18·40	16·55	0·5343	0·1348	17	0·054	0·997	8
Ethanol–ethanol monohydrate	**III**	18·86	18·81	18·18	0·04805	0·0355	8	0·047	0·997	8
Ethanol monohydrate–water	**III**	22·08	20·17	18·86	0·02509	16·29	17	0·220	0·995	8
Pyridine–water	**IVa**	27·51	27·22	25·00	0·3910	0·0378	11	0·059	0·990	3
Pyridine–water	**IVb**	22·99	22·41	19·55	0·4660	0·0341	11	0·038	0·994	3
Pyridine–water	**IVc**	21·28	20·19	16·39	0·5208	0·0444	11	0·038	0·998	3
Pyridine–water	**IVd**	20·51	19·38	14·08	0·5208	0·0683	11	0·086	0·996	3

[a] The experimental data are taken from the literature.[3,8]
[b] Number of experimental points.
[c] Correlation coefficient. See Table 4, footnote a.

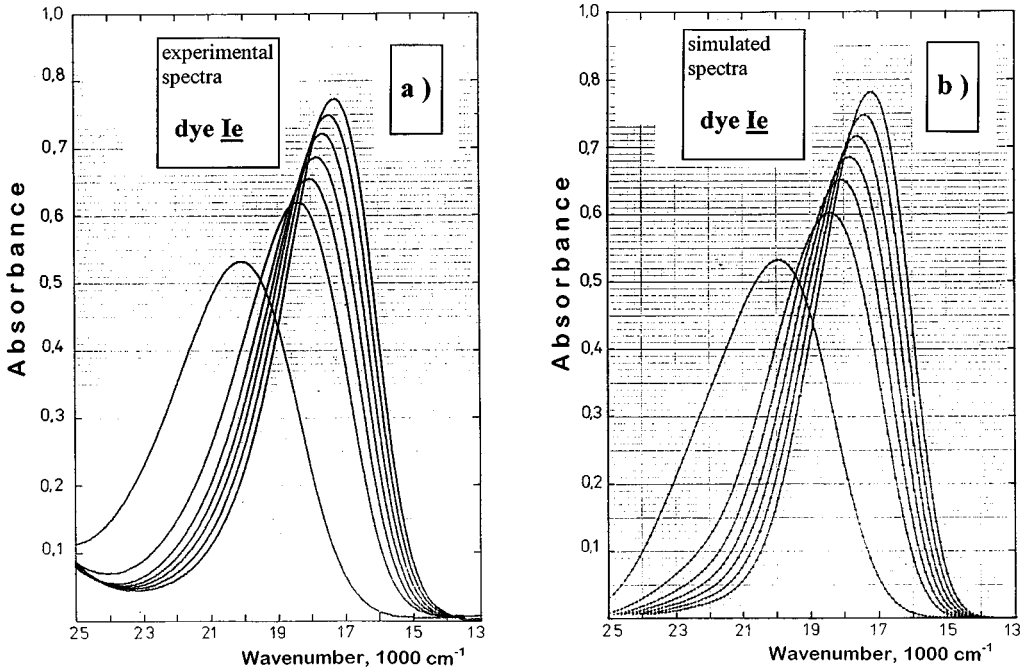

Figure 12. Fragment of (a) measured and (b) simulated UV–VIS absorption spectra of merocyanine dye **Ie** in the pyridine monohydrate–water subsystem for various molar fractions of water from 1·0 (the lowest curve) to 0·4 (the highest curve) at 0·1 intervals

tors applied for the study of some binary aqueous–organic mixtures. It is true, that the lack of possibility of finding a universal polarity scale for binary solvent mixtures resembles similar difficulties in searching for the philosopher's stone; however, proceeding according to the strategy of similarity models[27] gives a chance for the practical use of some derived values.

EXPERIMENTAL

Materials. Compounds **Ia–j** (see Scheme 2) were obtained by alkaline elimination of perchloric acid from 5-(3-R_1-4-hydroxy-5-R_2-phenyl)-7,7-dimethyl-7*H*-indolo[1,2-*a*]quinolinium perchlorates according to earlier reports.[28–30] The betaine **II** was prepared according to Dimroth *et al*.[2]

Solvents. The composition of binary solvent mixtures was determined according to the volume and density of the given components.

UV–VIS spectral measurements. All spectra were recorded at constant temperature (with ±0·1 K error) for mixtures of 1–3 μl of a DMSO solution of a dye (10% w/v dye concentration) in 2–3 ml of solvent. The final dye concentration was 1×10^{-5}–3×10^{-5} mol l^{-1}. Carl Zeiss Jena Specord UV–VIS and Specord M40 spectrophoto-

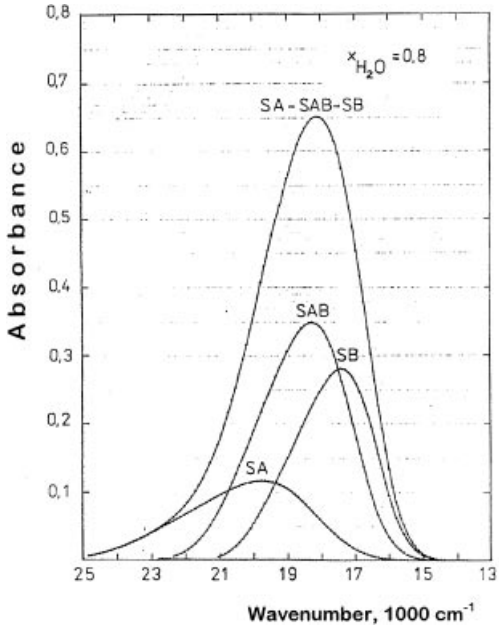

Figure 13. Simulated UV–VIS absorption band of merocyanine dye **Ie** dissolved in the pyridine monohydrate–water subsystem at a molar fraction of water $x=0{\cdot}8$. Shown are the component bands which correspond to the solvates SA (band on the left side), SAB (band in the middle) and SB (band on the right)

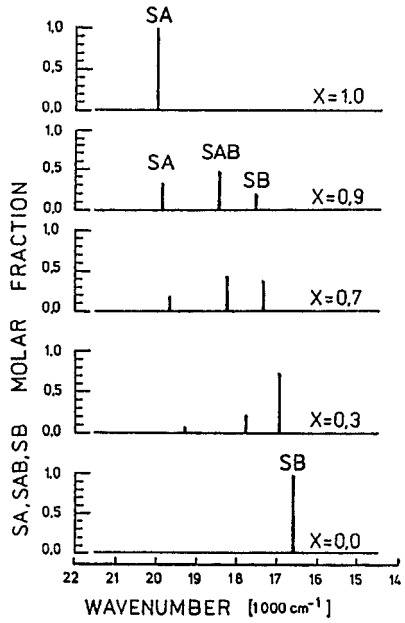

Figure 14. Positions and relative intensities of component bands for merocyanine dye **Ie** at various molar fractions of water

Table 6. Estimated parameters for the equilibrium constants for two dyes and two solvents (based on experiments at six temperatures, $\beta=0$)

	Solvent system			
	Acetonitrile–water		Pyridine monohydrate water	
	Dye **Ij**		Dye **Il**	
Parameter	For K_A	For K_B	For K_A	For K_B
Entropy ($J\,K^{-1}\,mol^{-1}$)	−1·03 ±0·47	−2·86 ±0·13	0·09 ±0·40	−5·22 ±0·55
Enthalpy ($J\,mol^{-1}$)	0·009 ±0·147	−0·647 ±0·041	0·271 ±0·125	−1·289 ±0·173
Correlation coefficient, *R*	0·033	0·992	0·734	0·966
Reciprocal of significance level ($1/\alpha$)	2	16 000	11	800
Student's *t*	0·07	15·72	2·16	7·47

meters were employed. They were equipped with 1 and 5 cm quartz cells. The maximum error of absorbance maximum determination was 20 cm^{-1}.

Calculations. Calculations were performed using the non-linear least-squares method. The parameters were determined with 0·01% accuracy. The significance level and its reciprocal were calculated numerically by the interpolation–extrapolation method, based on the critical correlation coefficient and the number of degrees of freedom.

Determination of K_A and K_B constants. The merocyanine dyes **Ia**–**j** are compounds which obey the earlier proposed VBHB model.[1,5] Therefore, they are assumed to take the hydrogen-bonded betaine form in their ground state in solutions consisting of solvents of polarity not lower than 200 kJ mol^{-1} on the E_T scale. Ethanol forms stable intersolvent associated molecules. Therefore, in spite of the polarity of the hydrates, which exceeds 210 kJ mol^{-1}, this solvent was rejected for our studies. A mixture of pyridine monohydrate (E_T=213·5 kJ mol^{-1}) with water (E_T=264·5 kJ mol^{-1}) appeared to be a suitable binary solvent system. For compound **Ij** (R_1=NO_2, R_2=H), a mixture of acetonitrile (E_T=192·6 kJ mol^{-1}) with water can be used because **Ij** is in the betaine form if the solvent polarity E_T is higher than 188·4 kJ mol^{-1}. The dyes **Ia**–**j**, having more intense solvent-sensitive absorption bands (log ε=4·5) than betaine **II** (log $\varepsilon\approx$3),[2] were more convenient for the investigations. The results of the measurements are given in Tables 1–3.

Simulation of the UV–VIS absorption spectra. For comparison of the experimental data with the values predicted by the presented model, dye **Ie** was used. The UV–VIS absorption spectra were measured for solutions with molar fractions of water varying from 0·4 to 1·0 at intervals of 0·1. Molar extinctions of the absorption bands in solution of pure pyridine monohydrate and in pure water were approximated by an envelope of n Gaussian curves which is expressed by the following equation:

$$\varepsilon_{(\bar{\nu})}=\varepsilon\alpha\sum_{i=0}^{n}\left(1-\frac{i}{i+n}\right)\exp\left\{-\left[\frac{x-\delta-\mathrm{iD}}{1\cdot201105(\sigma)}\right]^2\right\} \quad (28)$$

where α is a coefficient correcting the intensity of the band, n is the number of additional components of bands which cause their asymmetry, σ is the half-width measured from a maximum towards longer wavelength, D is the interval between particular components bands and δ are the differences between the wavenumber of the maximum of the envelope and the wavenumber of the most intense component of that band. Parameters were selected after determination of the asymmetry coefficient of the absorption band, measured at 2/3, 1/2 and 1/3 of intensity, and comparison with the tabulated values calculated for various combiantions of n, D and σ. The α and δ parameters are the theoretical corrections for a band amplitude and its position, respectively, when n, D and σ values are adopted. Corresponding parameters for the band of SAB solvate were estimated as the geometric weighted average according to the following general equation:

$$p_{AB}=p_A^{\theta}\,p_B^{1-\theta} \quad (29)$$

where

$$\theta=\frac{\bar{\nu}_{SB}-\bar{\nu}_{SAB}}{\bar{\nu}_{SB}-\bar{\nu}_{SA}} \quad (30)$$

All K_A, K_B and $\bar{\nu}_{SAB}$ values were determined numerically by the gradient method when β=0 and based on the $\{\bar{\nu}, x\}$ set. Determined in this way, K_A and K_B were repeatedly calculated, based on the same experimental data when β varied from 0·0 to 0·4 at intervals of 0·05. Taking into consideration the similarity of both the measured and calculated spectra, the best results were found for β=0·3. The following parameters were used:

ε_A=53·10, α_A=0·642, δ_A=−835 cm^{-1}, σ_A=1328 cm^{-1}, n_A=3, D_A=1360 cm^{-1};

ε_B=93·64, α_B=0·759, δ_B=−425 cm^{-1}, σ_B=915 cm^{-1}, n_B=2, D_B=1139 cm^{-1};

$\bar{\nu}_{SA}$=20 000 cm^{-1}, $\bar{\nu}_{SAB}$=17 990 cm^{-1}, $\bar{\nu}_{SB}$=16 600 cm^{-1};

K_A=0·373 l mol^{-1}, K_B=0·068 l mol^{-1}, β=0·3.

ACKNOWLEDGEMENTS

We thank Professor Piotr Tomasik of the Hugon Kołłątaj Academy of Agriculture, Cracow, for helpful discussions, Professor Jerzy Sotdek of the Shipbuilding Institute of our University for enabling us to perform numerical calculations and Mrs Teresa Cieszyńska for help with the measurements.

REFERENCES

1. J. A. Soroka, *Pol. J. Chem.*, **66**, 2025–2045 (1992).
2. K. Dimroth, C. Reichardt, T. Siepmann and F. Bohlmann, *J. Liebigs Ann. Chem.* **661**, 1–37 (1963).
3. S. Dähne, F. Schob, K. D. Nolte and R. Radeglia, *Ukr. Khim. Zh.* **41**, 1170–1176 (1975).
4. L. G. S. Brooker, G. H. Keyes, R. H. Sprague, R. H. Van Dyke, E. Van Lare, G. Van Zandt, F. L. White, H. W. J. Cressman and S. G. Dent, Jr., *J. Am. Chem. Soc.* **73**, 5332–5350 (1951).
5. K. B. Soroka and J. A. Soroka, *J. Phys. Org. Chem.* **4**, 592–604 (1991).
6. K. B. Soroka and J. A. Soroka, *Abstracts of Papers, Vth International Conference on Correlation Analysis in Organic Chemistry*, Paris, 1991, Abstract B-18.
7. K. B. Soroka, PhD Thesis, Technical University of Szczecin (1983).
8. C. Reichardt, *Solvents and Solvent Effects in Organic Chemistry*, 2nd ed. VCH, Weinheim (1988).

9. E. M. Kosower, *J. Am. Chem. Soc.* **80**, 3253–3260 (1958).
10. K. Dimroth and C. Reichardt, *Fresenius' Z. Anal. Chem.* **215**, 344–350 (1966).
11. H. Langhals, *Angew. Chem.* **94**, 739–749 (1982); *Angew. Chem., Int. Ed. Engl.* **21**, 724 (1982).
12. O. Pytela and M. Ludwig, *Collect. Czech. Chem. Commun.* **53**, 671–685 (1988).
13. M. Margules, *Sitzber. Akad. Wiss. Wien, Math. Naturw. Kl. II* **104**, 1243–1249 (1895).
14. R. D. Skwierzyński and K. A. Connors, *J. Chem. Soc., Perkin Trans. 2*, 467–472 (1994).
15. J. G. Dawber, J. Ward and R. A. Williams, *J. Chem. Soc., Faraday Trans. 1* **84**, 713–727 (1988).
16. M. Rosés, C. Ráfols, J. Ortega and E. Bosch, *J. Chem. Soc., Perkin Trans. 2* 1607–1615 (1995).
17. E. Bosch, M. Rosés, K. Herodes, I. Koppel, I. Leito and V. Taal, *J. Phys. Org. Chem.* **9**, 403–410 (1996).
18. J. Ortega, C. Ráfols, E. Bosch and M. Rosés, *J. Chem. Soc., Perkin Trans. 2* 1497–1503 (1996).
19. J. A. Soroka and K. B. Soroka, *Abstracts of Papers, Tenth International Conference on Physical Organic Chemistry*, Haifa, 1990, Abstract PO-B1, p. 209.
20. J. A. Soroka, *Fotochemia Hemicyjanin N-Aryloamoniowych, Prace Naukowe Politechniki Szczecińskiej, Dr. Sci. Theses* **505**, 92 (1993).
21. K. B. Soroka and J. A. Soroka, *Abstracts of Papers, IV Środowiskowa Konferencja Chemików*, Poznań, Poland, 1988, Abstract B-21.
22. M. Hida, H. Yoshida and S. Arai, *Sen'i Gakkaishi*, **42**, T74–T83 (1986); *Chem. Abstr.* **104**, 188/147w (1986).
23. W. M. Wiczk, T. Latowski, *Z. Naturforsch., Teil*, **A42**, 1290–1295 (1987).
24. M. Charton, *Prog. Phys. Org. Chem.* **13**, 119–251 (1981).
25. Y. Marcus and Y. Migron, *J. Phys. Chem.* **95**, 400–406 (1991).
26. Y. Migron and Y. Marcus, *J. Chem. Soc., Faraday Trans.* **87**, 1339–1343 (1991).
27. R. I. Zalewski, T. M. Krygowski and J. Shorter (Eds), *Similarity Models in Organic Chemistry, Biochemistry and Related Fields.* Elsevier, Amsterdam (1991).
28. K. B. Soroka and J. A. Soroka, *Pol. Pat.* 121 226 (1979); *Chem. Abstr.* **102**, 1849817 (1985).
29. K. B. Soroka and J. A. Soroka, *Tetrahedron Lett.* **21**, 4631–4632 (1980).
30. K. B. Soroka and J. A. Soroka, *Chem. Scr.* **29**, 167–171 (1989); *Chem. Abstr.* **113**, 61292v (1990).

